DivIVA phosphorylation affects its dynamics and cell cycle in radioresistant *Deinococcus radiodurans.*

Reema Chaudhary[a,b], Swathi Kota[a,b] and Hari S. Misra[a,b*]

[a]Molecular Biology Division

Bhabha Atomic Research Centre

Mumbai- 400085

[b]Life Sciences, Homi Bhabha National Institute

Mumbai- 400094

*Corresponding author

Dr Hari S Misra

Email: hsmisra@barc.gov.in

Tel: 91-22-269293821

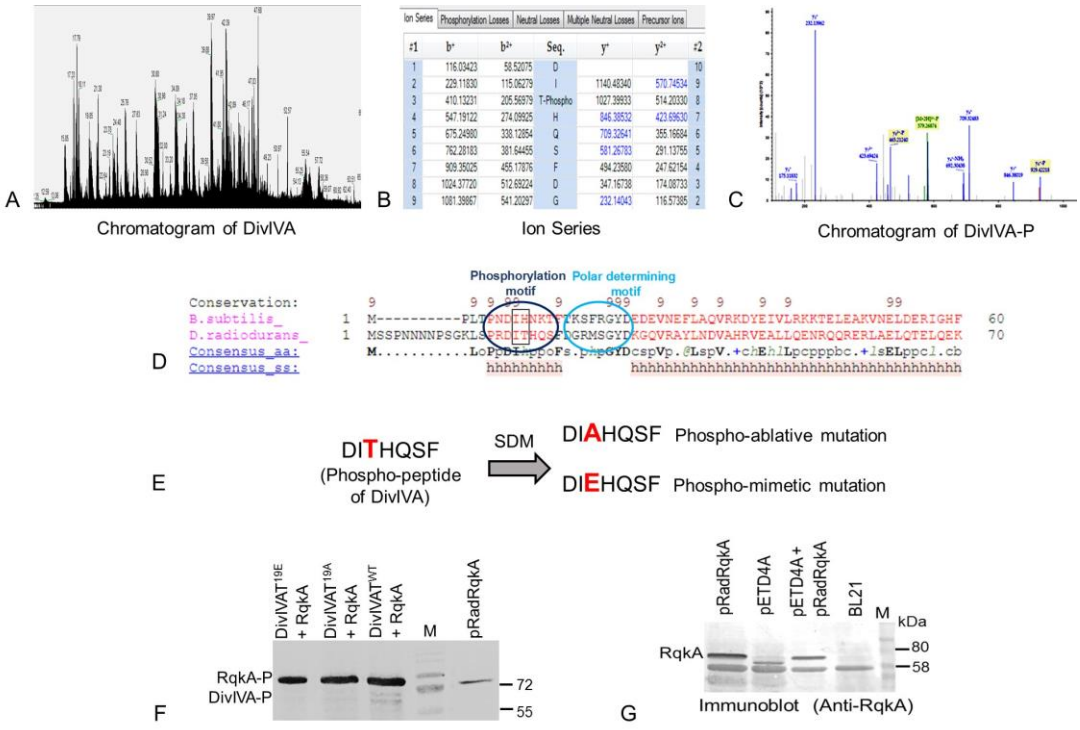

Figure S1

Fig. S1: Phospho-site mapping in deinococcal DivIVA. The phosphorylated drDivIVA protein was subjected to mass spectrometry for identification of the phosphosite. A chromatogram of the protein was generated, and ion series of the phospho-peptide fragment was also analyzed with respect to the non-phospho form of the protein **(A-B)**. The chromatogram has highlighted the phosphopeptide peaks **(C).** Pair-wise alignment of the first few amino acids of DivIVA of *B. subtilis* and *D. radiodurans* was highlighted to show the proximity of phosphorylation and polar motifs **(D).** Phospho-peptide was found to be DI***T***HQSFDGR, where T is mutated to alanine (A; phospho-ablative) and glutamate (E; phospho-mimetic) by site-directed mutagenesis **(E).** The mutant forms were also checked for phosphorylation *ex-vivo*. *E. coli* cells harbouring pRadRqkA and any one of the following plasmids: pRGD4A (DivIVA^{WT}), pRGD4A^{T19A} (DivIVA^{T19A}) and pRGD4A^{T19E} (DivIVA^{T19E}) were grown. The samples were run on 12% SDS-PAGE and immunoblotted with an anti-phospho Ser/Thr antibody**.** *E. coli* harbouring the pRadRqkA vector was used as a control **(F).** *E. coli* BL21 cells were co-transformed with pRadRqkA and pETD4A. Negative controls were only BL21 cells and cells harbouring either pRadRqkA or pETD4A. Expression of RqkA was confirmed by immunoblotting using an anti-RqkA antibody **(G).**

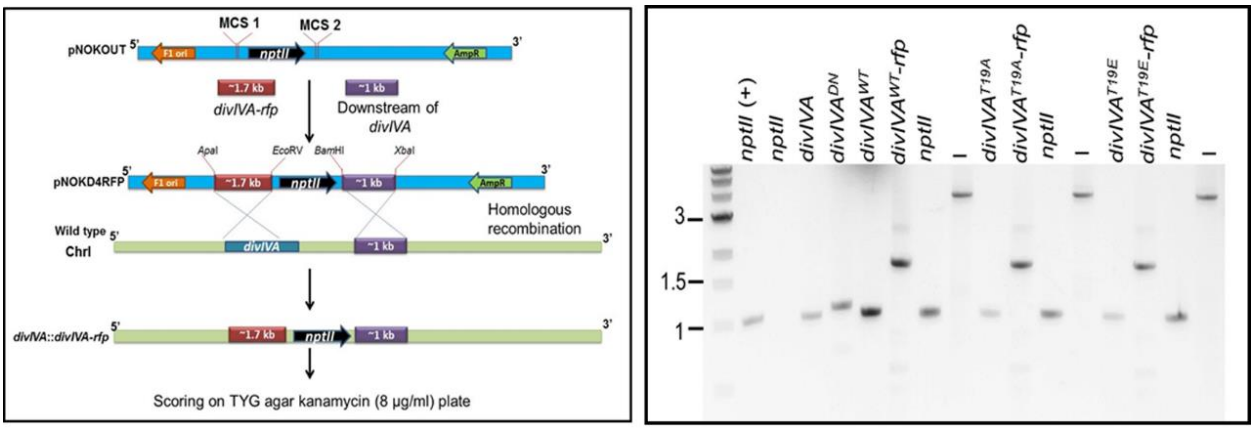

A B

Figure S2

Fig. S2. A diagrammatic representation of the strategy employed for replacement of *divIVA* with RFP fusions of wild-type and mutant alleles in the chromosome of *D. radiodurans*. The *divIVA-rfp* and downstream sequences of *divIVA* were cloned into the pNOKOUT vector, yielding pNKD4A **(A)**. The same strategy was followed for creating other mutant constructs, where *divIVA*^{T19A}*-rfp* and *divIVA*^{T19E}*-rfp* were cloned upstream of *nptII* in pNOKOUT, yielding pNKD4A^{T19A} and pNKD4A^{T19E,} respectively (A). The plasmids were linearized and transformed into *D. radiodurans* cells, and transformants were scored in the presence of kanamycin. The integration of *rfp* downstream to *divIVA* followed by antibiotic resistance marker gene (*nptII*) was confirmed by diagnostic PCR using primers as described in Table 1 **(B)**. The PCR products in the gel are labelled for their respective identity as follows: *nptII* (+) for antibiotic resistance gene from pNOKOUT; *nptII* from the corresponding knock-in strain; *divIVA* (from R1), *divIVA*^{WT} (from *divIVA::divIVA-rfp),* *divIVA*^{T19A} (from *divIVA::divIVA*^{T19A}*-rfp)* and *divIVA*^{T19E} (from D4A^{T19E} + DivIVA); *divIVA*^{DN} for downstream sequence of *divIVA; divIVA*^{WT}*–rfp, divIVA*^{T19A}*-rfp* and *divIVA*^{T19E}*-rfp* for *divIVA* along with *rfp* in all the three types of strains; I indicates the product of *divIVA-rfp-nptII-divIVA*^{DN} from the corresponding strains.

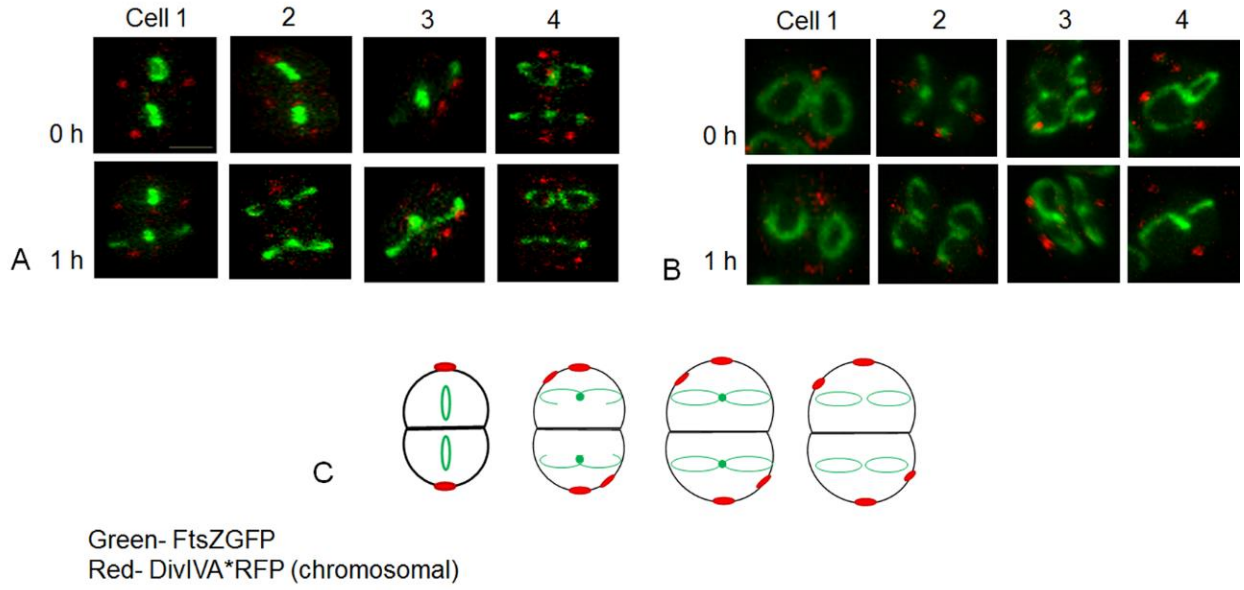

Figure S3

Fig. S3. Time course confocal microscopy of *D. radiodurans* expressing drDivIVA- and DivIVA^{T19A}-RFP from its native promoter and FtsZ-GFP. The *D. radiodurans* cells co-expressing DivIVA-RFP (A) or DivIVA^{T19A}-RFP (B) and FtsZ-GFP were processed for time-lapse microscopy, and cells were imaged for 3-4 h for every 1 h with a scale bar of 500 nm. The signal of drDivIVA-RFP has bleached after 1 h, so different cells were taken from the field and two time points (t = 0 and 1 h) are shown for respective cell to represent the dynamics of native DivIVA-RFP and stages like the closed, 3-shaped and intermediate stages of the FtsZ-GFP ring during cell division (C).